

## THE CNOC CLUSTER SURVEY

$\Omega$ ,  $\sigma_8$ ,  $\phi(L, z)$  Results, and Prospects for  $\Lambda$  Measurement

R. G. CARLBERG, H. K. C. YEE, H. LIN, C. W. SHEPHERD AND  
P. GRAVEL

*University of Toronto, Toronto ON, M5S 3H8 Canada*

E. ELLINGSON

*University of Colorado, CO 80309 USA*

S. L. MORRIS, D. SCHADE, J. E. HESSER, J. B. HUTCHINGS AND  
J. B. OKE

*National Research Council of Canada, Herzberg Institute of  
Astrophysics, Dominion Astrophysical Observatory, Victoria,  
BC, V8X 4M6, Canada*

R. ABRAHAM

*Institute of Astronomy, Cambridge CB3 OHA, UK*

M. BALOGH, G. WIRTH, F. D. A. HARTWICK AND C. J. PRITCHET  
*University of Victoria, Victoria, BC, V8W 3P6, Canada*

AND

T. SMECKER-HANE

*University of California, Irvine, CA 92717, USA*

**Abstract.** Rich galaxy clusters are powerful probes of both cosmological and galaxy evolution parameters. The CNOC cluster survey was primarily designed to distinguish between  $\Omega = 1$  and  $\Omega \simeq 0.2$  cosmologies. Projected foreground and background galaxies provide a field sample of comparable size. The results strongly support a low-density universe. The luminous cluster galaxies are about 10-30% fainter, depending on color, than the comparable field galaxies, but otherwise they show a slow and nearly parallel evolution. On the average, there is no excess star formation when galaxies fall into clusters. These data provide the basis for a simple  $\Lambda$  measurement using the survey's clusters and the field data. The errors in  $\Omega_M$ ,  $\Omega_\Lambda$ ,  $\sigma_8$  and galaxy evolution parameters could be reduced to a few percent with a sample of a few hundred clusters spread over the  $0 < z < 1$  range.

## 1. The $\Omega$ Problem

The total mass-to-light ratio of field galaxies multiplied with the field luminosity density gives, by definition, the mean mass density of the universe,  $\rho_0$  (Oort 1958; Gunn 1978). The complications in the measurement are to provide unbiased mass estimates and to measure any luminosity difference between the galaxies for which total system masses are known and field galaxies. Small, dense systems, like individual galaxies and small groups, exhibit “luminosity segregation” where the luminosity distribution is more concentrated than the mass distribution (Bahcall, Lubin & Dorman 1995). The largest virialized structures — rich clusters — indicate  $\Omega \simeq 0.2 - 0.4$ , but these measurements may be biased by luminosity segregation and differential evolution of the very red cluster galaxies as compared to bluer field galaxies. On even larger scales, where overdense structures are still expanding, but retarded from the Hubble flow, bulk flows of galaxies measure the parameter  $\Omega^{0.6}/b$ , where  $b$  is the assumed linear bias,  $b = (\delta n/n)/(\delta \rho/\rho)$ , relating the tracer galaxy number densities and the mass field density. The flow measurements tentatively indicated  $\Omega \simeq 1$  (Dekel 1994; Strauss & Willick 1995), but recent increases in sample size and new analyses indicate possible compatibility with  $\Omega \simeq 0.2 - 0.4$  (Fisher *et al.* 1994; Davis, Nusser & Willick 1996; Willick *et al.* 1996). The value  $\Omega = 1$  is of considerable interest as the “natural” value (the “Dicke coincidence”) for a universe that has expanded many e-folds, and as the value originally predicted by inflationary cosmology (Guth 1981; Bardeen, Steinhardt & Turner 1983; Turner 1995). If  $\Omega = 1$  and all the dark matter falls into clusters along with galaxies (as it must if it is collisionless and cold), then rich clusters, which draw their mass from regions  $10h^{-1}$  Mpc in radius, must have a total virialized mass-to-light ratio,  $M_v/L$ , about 2.5 to 5 times higher than the standard virial analysis gives. The cluster data did not rule out such high  $M/L$  values in the field, due to unconstrained systematic errors in both  $M_v$  and  $L$ .

The Canadian Network for Observational Cosmology (CNOC) sample was designed to create a dataset that allows complete internal control of most aspects of the cluster  $\Omega$  estimate, especially luminosity segregation and differential evolution of cluster galaxies relative to the field. The cluster sample was chosen from the Einstein Medium Sensitivity Survey Catalogue of X-ray clusters (Gioia *et al.* 1990; Henry *et al.* 1992; Gioia & Luppino 1994) to have a high X-ray luminosity, which helps guarantee that the clusters are reasonably virialized, suggests that they will contain many galaxies, and allows other cosmological measurements. The sample was augmented with A2390 to fill an RA gap. The clusters are at  $z \sim 0.3$  so they have a significant redshift interval over which the surround-

ing field galaxies are nearly uniformly sampled in redshift. Observations were made at CFHT in 24 assigned nights in 1993 and 1994, of which 22 were usefully clear. The primary catalogues contain Gunn  $r$  magnitudes and  $g - r$  colors for 25,000 objects, plus radial velocity measurements at an average accuracy of  $100 \text{ km s}^{-1}$  (Yee, Ellingson & Carlberg 1996) for a subsample of 2600. All results are reported for  $H_0 = 100 \text{ km s}^{-1} \text{ Mpc}^{-1}$  and  $\Omega_0 = 0.2$ ,  $\Omega_\Lambda = 0$ .

The overall CNOC program is encapsulated as follows:

- select clusters from an unbiased X-ray catalogue of large  $z$  range,
- observe clusters out to a radius with overdensity of  $200\rho_c$  or lower,
- measure virial mass-to-light ratio,
- test and correct virial mass,
- test for  $z$  dependence of  $M_v/L$ , measure  $\phi(L, z)$  for clusters,
- measure  $\phi(L, z)$  for the field sample,
- measure  $n(> M, z)$ , the cosmological density of clusters, and,
- measure the evolution of field clustering and clustering velocities.

The main results from this ongoing program of investigation are summarized below but discussed in detail in a series of papers. The observational methods, which are designed to efficiently measure redshifts of galaxies in the primary sample, are discussed in Yee, Ellingson & Carlberg (1996). The measurement of global quantities, such as the velocity dispersion and virial mass-to-light ratio, is done in Carlberg, *et al.* (1996). The average mass and light profiles are compared in Carlberg, Yee & Ellingson (1997) to measure the biases of the virial mass-to-light ratio and correct the luminosities of cluster galaxies to field galaxy values. Carlberg, *et al.* (1997a) shows that the same mass profile can be recovered from two independent and very different subsamples of the cluster data. The average mass profile is compared to a theoretical prediction in Carlberg, *et al.* (1997b), finding an impressive agreement. The sample was designed such that the amplitude of the primordial density fluctuation spectrum could be measured on cluster scales, with the results given in Carlberg, *et al.* (1997b). Some preliminary results of the CNOC field survey, now comprising about 2/3 of the 5000 primary sample redshifts, are given below.

## 2. CNOC Cluster Masses

The virial mass is  $M_v = 3G^{-1}\sigma_1^2 r_v$ , where  $\sigma_1$  is the line-of-sight velocity dispersion and  $r_v$  is the virial radius of the observed galaxies (Binney & Tremaine 1987). Deciding which galaxies in redshift space are cluster members is fundamentally ambiguous. That is, a cluster galaxy with a completely reasonable line-of-sight velocity of  $1000 \text{ km s}^{-1}$  appears in redshift space at  $10h^{-1} \text{ Mpc}$  from the cluster's center of mass, far outside the

virialized cluster and intermingled with field galaxies. This complication increases in severity as the cluster density declines with projected distance from the cluster center where our sample is specifically intended to probe. Our straightforward solution to this problem is to subtract the mean density of field galaxies in redshift space from the redshift space of the cluster (Carlberg *et al.* 1996). The resulting velocity dispersions are about 13% lower than precisely the same cluster data give without background subtraction. Gratifyingly, our velocity dispersions are in excellent agreement with those inferred from the mean X-ray temperatures (Mushotzky & Scharf 1997). Our estimate of  $r_v$  uses a “ringwise” estimate, rather than the traditional “pointwise” estimate (Binney & Tremaine 1987). This allows us to include a selection function for the roughly rectangular window on the sky which outlines the fields and it helps to reduce noise in the estimated virial radius. The ringwise estimator overestimates the virial radius of the clusters because it does not account for their flattening. We use the mean of the ratio of the ringwise to the pointwise estimator, which is about 1.28, to make this correction. The ringwise estimator includes a small “softening”, of one arcsec, to avoid a divergence when two galaxies are at the same radius.

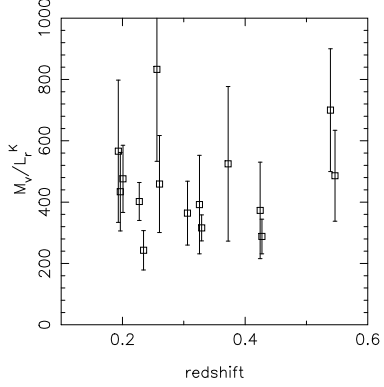


Figure 1: The virial mass-to-light ratios as a function of redshift. The luminosities have been k-corrected and allow for evolution at the rate of  $M_*(z) = M_*(0) - Qz$ , with  $Q = 1$ . The 15 clusters are consistent with having a universal  $M_v/L(0) = 374h M_\odot/L_\odot$  with the same dataset giving a closure value  $1502h M_\odot/L_\odot$ , both with 10% standard errors.

The total galaxy luminosity of the cluster galaxies in ratio to  $M_v$  gives  $M_v/L$ , an estimate of the total mass-to-light ratio. The average k-corrected Gunn  $r$   $M_v/L$ , for  $M_r^k \leq -19$  mag but integrated to infinity with the luminosity function ( $M_* = -20.3$  mag,  $\alpha = 1.1$ ), is  $289 \pm 50h M_\odot/L_\odot$  at  $z = 0.31$ . If corrected for pure luminosity evolution at the rate of 1 magnitude of brightening per unit redshift the mean Gunn  $r$   $M_v/L$  extrapolates to  $374 \pm 54h M_\odot/L_\odot$  at redshift zero. The mean standard error per cluster on average is 40%, although this can be reduced to 25% by eliminating the clusters with large errors. A major result is that  $M_v/L$  is the same for all clusters once minimal passive evolution of the cluster galaxies is taken into account (Carlberg *et al.* 1996). For the 15 clusters displayed in Figure 1  $\chi^2 = 16.6$  which is about 28% probable for  $\nu = 14$  degrees of freedom, that is, consistent with no intrinsic variation. X-ray (David, Jones, & Forman

1995) and weak lensing analyses (Tyson & Fischer 1995; Squires *et al.* 1996; Smail *et al.* 1997; Fischer & Tyson 1997) generally find results in accord with these.

### 3. Mass Profiles and Virial Mass Bias

Our observations extend over what is expected to be the entire virialized volume of the cluster. Analytic models (Gott & Gunn 1972) and simulations (Cole & Lacey 1996) find that the virialized mass is generally contained inside the surface where the mean interior density is approximately  $200\rho_c$ , which defines the radius  $r_{200}$ . The small extrapolation from the observationally derived  $r_v$  to  $r_{200}$  assumes  $M(r) \propto r$ , which gives  $r_{200} = \sqrt{3}\sigma_1/[10H(z)]$ , where  $H(z)$  is the Hubble constant at redshift  $z$ .

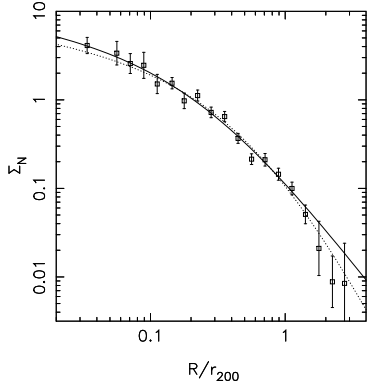


Figure 2: The background subtracted surface density profile, fitted with NFW (solid line) and Hernquist (dotted line) functions, both of which are statistically acceptable. The mass is accurately traced with this profile, as shown below. The remarkable result is that the NFW prediction of the scale radius is completely in accord with our measurements.

The accuracy of the virial mass depends on the tracer galaxies having the same distribution as the mass. We compare the light-traces-mass profile,  $M_L(r) = L(r) \times M_v/L$ , to the dynamical mass profile,  $M_D(r)$ , derived from the Jeans Equation,

$$\frac{\sigma_r^2}{r} \left[ \frac{d \ln \sigma_r^2}{d \ln r} + \frac{d \ln \nu}{d \ln r} + 2\beta \right] = -\frac{GM_D(r)}{r^2}, \quad (1)$$

where  $\beta = 1 - \sigma_\theta^2/\sigma_r^2$  is the velocity anisotropy parameter. This equation does not depend on the density of the tracer galaxies,  $\nu(r)$ , following the mass density profile,  $\rho(r)$ .

To create an effectively spherical cluster and to reduce the effects of substructure, all the cluster galaxies are combined into one “ensemble” cluster by normalizing the velocities to  $\sigma_1$  and the projected radii to the  $r_{200}$  value of each cluster. The two quantities measured from this distribution are the surface number density profile of cluster galaxies,  $\Sigma_N(R)$ , shown in Figure 2, and the projected velocity dispersion profile, Figure 3. The volume number density profile is modeled as  $\nu(r) = A/[r(r + a)^p]$ , where

$p = 2$  for the Navarro, Frenk & White function (1997, hereafter NFW) and  $p = 3$  for Hernquist's (1990) form.

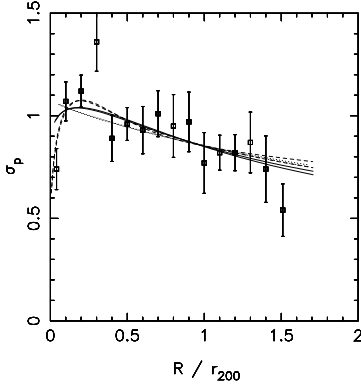


Figure 3: The projected velocity dispersion profile and the projection of the fitted profiles, for a range of  $\beta$  and  $[c_1, c_2]$ . See Carlberg *et al.* 1997d for details.

The radial velocity dispersion is modeled as  $\sigma_r^2 = B[c_1r/(1 + c_1r) + c_2]/[1 + r/b]$ , where  $B$  and  $b$  are the two parameters adjusted to fit the observed  $\sigma_p(R)$ . The  $c_1$  and  $c_2$  parameters are externally fixed to vary the shape of the curve. The velocity anisotropy is taken as an approximate fit to the results of n-body simulations. A range of  $\sigma_r(r)$  fits are shown in Figure 3. The resulting ratio,  $b_{Mv}(r) = M_D(r)/M_L(r)$  shown in Figure 4, is not very sensitive to the details of the velocity modeling.

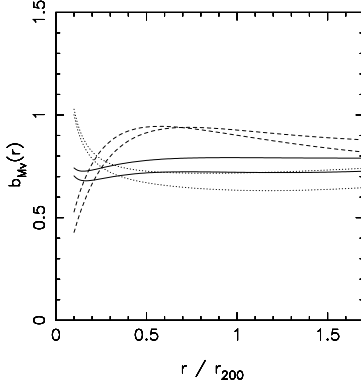


Figure 4: The derived ratio of the dynamical mass profile,  $M_D(r)$ , to  $r$  selected galaxy profile,  $L(r)$ , normalized with the virial mass-to-light ratio evaluated inside  $1.5r_{200}$ . In each pair of curves the upper line at small radius is for  $\beta_m = 0.3$  and the lower for  $\beta_m = 0.5$ . The dotted line is for  $c_1 = 0$ , the dashed for  $c_2 = 0$  and the solid line is our preferred  $c_1 = 8, c_2 = 1/2$ .

There are two conclusions to be drawn from Figure 4. First, over a range of about two decades of projected density or three decades of volume density, the integrated galaxy distribution traces the mass distribution to an accuracy of about 20% or better. Second, the virial mass is always an overestimate of the true mass contained within that radius, which we estimate to be a factor  $0.82 \pm 0.14$ . We attribute the mass overestimate of  $M_v$  to dropping the surface pressure term at  $P_s = 0$  in the virial theorem, *i.e.*  $2T + W = 3P_sV$ . Simple modeling of an equilibrium cluster shows that truncating the data at  $r_{200}$  will cause  $M_v$  to be upward biased at the 15-25% level that is inferred from the Jeans Equation.

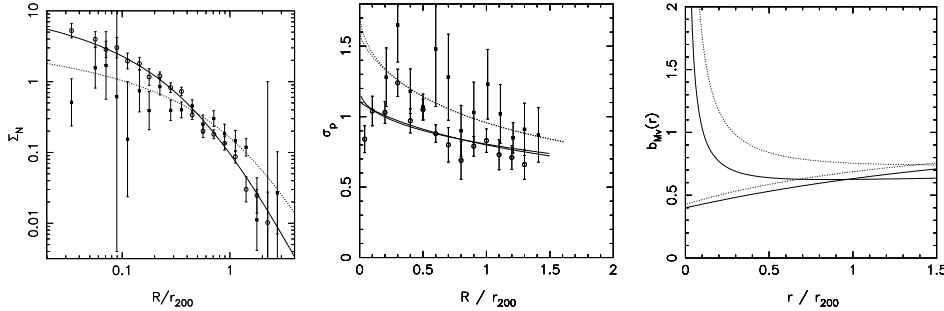


Figure 5: The projected number density profiles (left panel) and velocity dispersion profiles (middle panel) of the blue (solid squares and dotted lines) and red (circles and solid lines) cluster galaxies. They yield *identical* mass profiles (right panel) near  $r_{200}$ , where the upper pair of lines are for  $\beta = 0$  and the lower pair are for  $\beta = 0.5$ .

Splitting the cluster sample into independent blue and red subsamples demonstrates that the clusters are effectively in equilibrium and that the results are robust for drastically different samples. These two subsamples also illustrate the perils of the virial mass estimator. The blue galaxies are about twice as extended and have a 20% higher velocity dispersion than the red galaxies, Figure 5. Consequently the blue galaxies indicate a virial mass about three times larger than the red galaxies give. However each of these subsamples independently gives the same mass profile from the Jeans equation as found from the full sample, which we take as strong support for the assumption that both subsamples are effectively in equilibrium with the cluster potential (Carlberg *et al.* 1997a). It should be noted that galaxies with red colours are somewhat more concentrated than the total mass distribution, so the procedure of comparing the mass profile to the “red-sequence” light profile is likely to give a rising mass-to-light ratio.

The scale radius,  $a$ , is predicted to be a relatively large 0.20–0.26 of  $r_{200}$ , for simulations normalized to the observed cluster cosmological density, but otherwise the prediction is relatively insensitive to cosmological parameters (NFW). It is a significant success of the generalized CDM model that the observed scale radius  $a = 0.13 – 0.43$  (95% confidence) is in complete accord with NFW’s prediction.

#### 4. Normalization of the Density Perturbation Spectrum, $\sigma_8$

The normalization of the density fluctuation spectrum is fundamental to all predictions of structure formation. The parameter  $\sigma_8$  is the variance of the linear density perturbation spectrum in  $8h^{-1}$  Mpc spheres. The CNOC cluster sample and observational strategy (Yee, Ellingson & Carlberg 1996) were specifically designed to produce data useful for a  $\sigma_8$  measurement.

The sample's primary advantage is that the cluster masses are accurately known near the virial radius, which is essential for a reliable estimate of the linear mass scale from which the cluster collapsed. We combine our data with similarly selected clusters from the EMSS (Henry *et al.* 1992) and ESO Cluster surveys (Mazure *et al.* 1996) to extend the redshift range of the cosmological density estimates. The cluster cosmological density data are modeled (Press & Schechter 1974) to constrain the  $\sigma_8 - \Omega$  pair. It is not observationally straightforward to give accurately the full virialized mass of a cluster, but it is straightforward to extrapolate the mass inside some specified aperture, conventionally the Abell radius,  $1.5h^{-1}$  Mpc. The measurement of cluster mass inside a fixed aperture is effectively a mass weighted velocity dispersion or temperature.

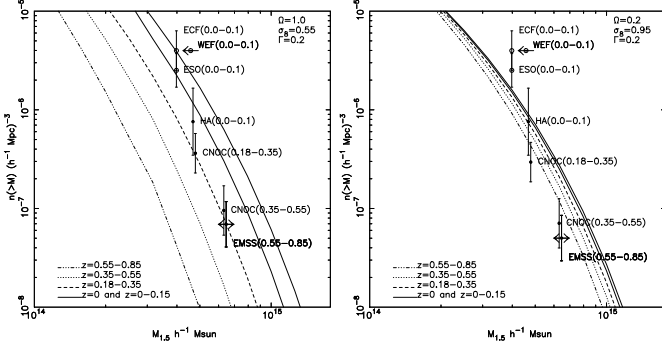


Figure 6: The measured cosmological density evolution of galaxy clusters with  $\Omega = 1$  (left) and  $\Omega = 0.2$  (right) predictions.

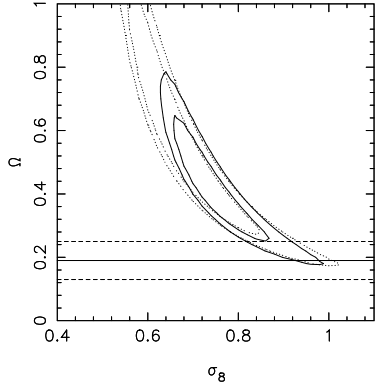


Figure 7: A plot of  $\chi^2$  for all independent samples (solid lines) and excluding the high redshift EMSS sample (dotted lines). The contours are the 90% and 99% confidence levels. The results of the CNOC analysis,  $\Omega = 0.19 \pm 0.06$ , with its  $1\sigma$  range are indicated.

The measured redshift change of the cosmological density of clusters, having  $\sigma_1 \gtrsim 800 \text{ km s}^{-1}$  requires some small corrections for the effects of X-ray selection, which are incorporated in the data of Figure 6. The analysis is greatly simplified because the  $L_x - \sigma_1$  relation has no detectable redshift evolution, as is also seen in the X-ray temperatures (Carlberg *et al.* 1997b; Mushotzky & Scharf 1997). The cluster cosmological density data are best described with  $\sigma_8 \simeq 0.75 \pm 0.1$  and  $\Omega \simeq 0.4 \pm 0.2$  (90% confidence), Figure 7. Taking the  $\Omega$  from cluster dynamical analysis as  $\Omega = 0.2$ , we find  $\sigma_8 =$

$0.95 \pm 0.1$  (90% confidence). The predicted cluster density evolution in an  $\Omega = 1$  CDM model exceeds that observed at  $z > 0.5$  by more than an order of magnitude, as shown in Figure 6.

## 5. Galaxy Evolution

It is essential for  $\Omega$  measurement to understand the differential evolution of cluster galaxies relative to field galaxies. The cluster galaxy population is on the average redder than the field, but the cluster population has an increasing blue fraction with redshift (Butcher & Oemler 1984). The origin of the blue cluster population has three basic possibilities. One possibility is cluster galaxies formed in a different way than field galaxies, with fundamentally different star formation rates at all epochs. However, hierarchical clustering leads one to expect that cluster galaxies originated in the field, and hence share a similar early star formation history which is altered in some way upon entry into the cluster. Ultimately star formation is greatly suppressed in cluster galaxies: however, there are two routes to this state. Either there was a burst of star formation upon entry into the cluster which largely exhausted the galaxy's gas supply, or, the gas was simply swept out of the galaxy (Baade & Spitzer 1951; Gott & Gunn 1972).

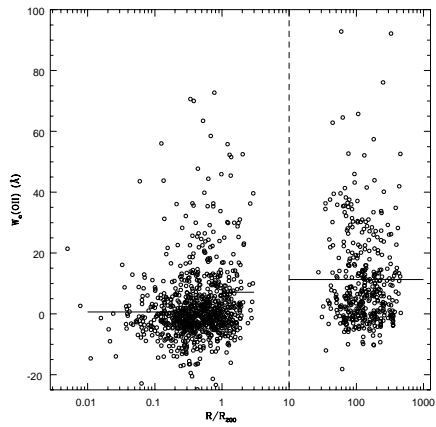


Figure 8: The radial dependence of the equivalent width of [OII] for galaxies with  $M_r^k \leq -18.5$  (Balogh *et al.* 1997 in preparation). The lines give the mean values in various radial ranges. Nowhere do cluster galaxies show an excess of star formation over the field.

In Figure 8 we show the equivalent width of the [OII]3727Å line as a function of radial distance from the cluster center, which is the projected distance in the inner region and the redshift space distance for the field galaxies. The sample is limited at a common  $M_r^k \leq -18.5$  mag, with an additional cut to eliminate low signal-to-noise spectra. The measured equivalent width implies a mean star formation rate of approximately  $0.05h^{-2} M_\odot \text{ yr}^{-1}$  in our clusters (Kennicutt 1992). Over  $10^{10}$  years this will add only a few percent stellar mass to the relatively high luminosity galax-

ies in our sample. Of particular note is that there is no evidence for a significant increase in star formation rate at any radius. Clusters do contain objects with strong emission lines, mostly near the cluster “edge”, but these are rare compared to the field. We conclude that the difference between cluster and field galaxy evolution is that star formation is truncated upon the entry of galaxies into the cluster (Couch & Sharples 1987; Abraham *et al.* 1996).

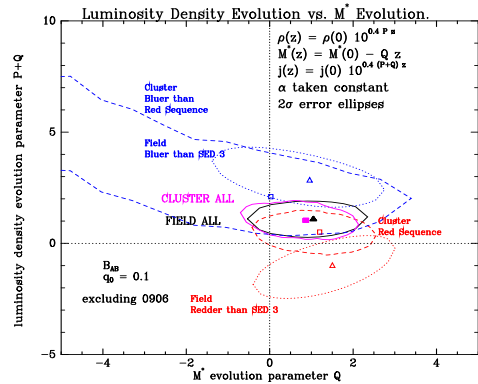


Figure 9: The  $B_{AB}$ -band evolution of  $M_*$  and  $j$  in magnitudes per unit redshift (Lin *et al.* 1997 in preparation). The solid lines give the 95% confidence contours for the full samples. The dotted and dashed lines are for blue and red subsamples. The cluster data are, unsurprisingly, consistent with passive evolution. The field galaxy evolution is nearly identical to the cluster galaxy evolution.

The evolution of the cluster galaxy population should be dominated by a passively evolving stellar population. The CNO survey has the advantage that the masses derived for each cluster can be used to normalize the luminosity functions of each cluster so that the redshift evolution of  $L/M$  can be measured. The evolution of the parameters of Schechter fits to the luminosity functions of galaxies having  $M_B(AB)$  more luminous than approximately  $-17$  mag is shown in Figure 9. The  $Q$  parameter measures the evolution of  $M_*$  with redshift (the faint end slope is held fixed at  $\alpha = -0.83$ , the best fit value) as  $M_* = M_*(0) - Qz$ . The evolution of the luminosity density,  $j(z)$ , is nearly statistically orthogonal to  $M_*$ . We model  $j(z)$  as an evolution in magnitudes,  $j(z) = j(0)10^{0.4(P+Q)z}$ . These luminosity function and evolution parameters are found using a parametric maximum likelihood technique (Sandage, Tammann & Yahil 1979; Saunders *et al.* 1990) applied to 1838 field galaxies and 1018 cluster galaxies above the sample limits.

We find that to a good approximation the density evolution parameters  $P \simeq 0.17$  (consistent with zero) indicating that there is little density evolution of cluster galaxies, as we expect for these high velocity dispersion clusters where merging and star formation are insignificant. We find  $Q \simeq 0.87$ , which in accord with predictions of purely passive evolution of a predominantly old stellar population of current at  $\sim 15$  Gyr today. In the field ( $\alpha = -0.93$ ), we find  $Q \simeq 1.05$  and  $P \simeq 0.04$ , nearly identical to the cluster values. Nearly identical values are inferred from this approach to the analysis of the CFRS data (Lilly *et al.* 1995; Lin, *et al.* 1997;

Lilly *et al.* 1996). The mean field star formation rate that we infer from [OII] over the  $0.2 \leq z \leq 0.6$  interval is only about  $0.3 M_{\odot} \text{ yr}^{-1}$  for galaxies more luminous than  $0.2L_*$  with a weak redshift dependence. This low mean star formation rate would add about 5-10% more stellar mass to an  $M_*$  galaxy (close to the sample mean and median) over this redshift interval, consistent with a mild field luminosity evolution and a modest difference between cluster and field. These results are supported by direct, cosmological model independent, measurements of the surface brightness of the galaxy spheroids and disks (Schade *et al.* 1996a; 1996b).

We conclude that field galaxies evolve roughly in parallel to cluster galaxies, although cluster galaxies have lower luminosity  $M_*$ , by  $0.3 \pm 0.1$  mag in B, or using different procedures,  $0.11 \pm 0.05$  mag in  $r$ . Simple stellar population modeling for truncated star formation shows that this is consistent with the mean colour difference of about 0.2 mag. The fading of cluster galaxies relative to the field is an essential, but relatively small, correction in the  $\Omega$  estimate. We interpret the Butcher-Oemler effect as likely being the result of blue, star forming, field galaxies falling into clusters at a rate that increases with redshift, although this remains to be quantified and tested.

## 6. A Neo-Classical $\Lambda$ Estimator

Cluster data allow a measurement of the geometry of the universe, using the following procedure. The mass density of the universe,  $\rho_0$ , is a conserved quantity which is estimated with the product of  $M/L(z)$  and  $j(z)$ . The  $M/L(z)$  is estimated from the clusters, with a relatively small correction, 10-30%, to allow for differential evolution with respect to the field. The luminosity density,  $j(z)$ , involves the volume element, which is strongly  $q_0$  dependent. If these quantities are calculated using the values of  $\Omega_0$  and  $\Omega_{\Lambda}$  that the real universe has, then  $\rho(z) = M/L(z) \times j(z)$  will be constant at  $\rho_0$ . However, if the “wrong” values are assumed, then the calculated  $\rho(z)$  will be dependent on redshift. For instance, if we assume that  $\Omega_0 = 1$ , but in fact  $\Omega_0 = 0.2$ ,  $\Omega_{\Lambda} = 0.8$ , then  $\rho(z)$  will rise 76% from  $z=0.2$  to  $z=0.8$ , which is easily detectable in samples of the CNOC size but having a larger redshift range. Note that this effect exceeds the entire differential evolution between field and cluster by a factor of two, and that the redshift variation in the differential evolution is even smaller. Although we will correct for galaxy evolution effects, they are small compared to the geometry changes we are trying to measure.

## 7. Discussion and Future Directions

The main goal of the CNOC survey is to use clusters of galaxies to derive a value of  $\Omega_0$  with a well determined error budget. The major innovation of our analysis is that it is completely self-contained, with the key assumptions being testable, and that the error estimates are derived from the data themselves. The dominant source of error is random cluster-to-cluster variations, rather than the internal error from individual clusters. The global mass-to-light ratio (in our photometric system, at mean redshift of  $z = 0.31$ , with k-corrections, but without evolution corrections) of our sample clusters of galaxies is constant within our typical errors of 25% at a value of  $289 \pm 50h M_\odot / L_\odot$ . Over the same redshift range we measure the closure value,  $\rho_c/j$ , to be  $1136 \pm 138h M_\odot / L_\odot$  (Carlberg *et al.* 1996). After allowing for the  $0.11 \pm 0.05$  mag lower luminosities of cluster galaxies and reducing  $M_v$  by  $0.82 \pm 0.14$ , we find that  $\Omega_0 = 0.19 \pm 0.06$ . In an independent luminosity function analysis, the evolution corrected  $B_{AB}$  value of  $M_v/L$  leads to  $\Omega_0 \simeq 0.23$  with a similar error budget.

There are no variations of the radial mass-to-light profile within the clusters, nor is there any variation with redshift. This requires any additional form of dark matter to be sufficiently hot that it does not fall into clusters, but perhaps participates in large scale flows. This is a very narrow parameter range and produces trouble for the evolution of the density perturbation spectrum. The most likely form of additional mass-energy, if it exists, is in the form of  $\Lambda$ , which additional cluster plus field observations in a neo-classical volume-redshift test can easily detect.

Two aspects of the cluster mass evolution are particularly satisfying. The derived  $\Omega_0$  accurately predicts the observed evolution of cluster cosmological density. With our value of  $\Omega_0$  we find that  $\sigma_8 = 0.95 \pm 0.1$ . Moreover the same  $\Omega$  in a cool, dark matter dominated universe, predicts remarkably accurately the “morphology” of the clusters, at least as encapsulated in the NFW results for the mean mass profile. For this low density cosmology the measured rate of both structural evolution, Figure 10 (Carlberg *et al.* 1997c), and galaxy evolution, Figure 9, over our redshift range is consistent with a formation “freeze out” at some  $z > 1$ , and possibly much higher.

There are considerable opportunities to refine and extend these results in a number of different directions. For the current sample these include improved coverage at  $1-3r_{200}$  to constrain the luminosity profile at large radius, which would lead to a tighter comparison with the core radius predictions and the slope at large radius. The same data would advance the empirical study of how field galaxies are altered upon infall into the cluster. The turnaround radius is at about  $5r_{200}$ . If the sample extended to pro-

jected radii well beyond turnaround, then there would be a clear measurement of the infall into the cluster, which is a “bulk flow”, hence measures the  $\beta = \Omega^{0.6}/b$  parameter. Such a measurement would directly compare the cluster  $\Omega$  estimate with a field  $\Omega^{0.6}/b$  measurement to resolve the large scatter present in the current estimates from flows. At these large radii many of the galaxies would be distant field galaxies, but their immense value is to provide a good estimate of the unperturbed background density, which is an essential ingredient in the measurement. Including the four high redshift EMSS clusters would allow an  $\Omega_\Lambda$  measurement with a precision of about  $\Delta\Omega_\Lambda \simeq 0.25$  to be made. With an efficient multi-object spectrograph on a 4 meter telescope, it takes 1-2 nights to observe a cluster at  $z \simeq 0.8$ .

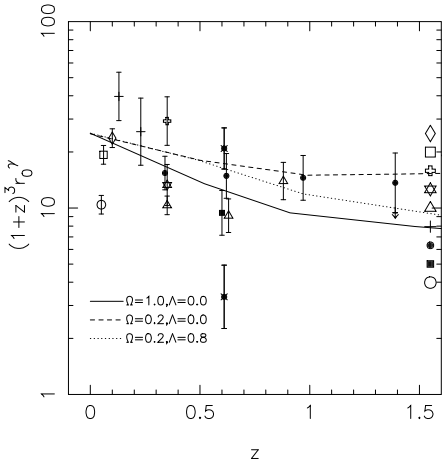


Figure 10: The evolution of the physical density of clustering with redshift from various samples. Red galaxies are more correlated than blue ones, notably the K-Keck (Carlberg *et al.* 1997c) and CNOC2 field (Shepherd *et al.* 1997, in preparation) samples. There is no compelling evidence for any change of physical density of clustered galaxies with redshift.

More ambitiously one can imagine in the near future assembling much larger cluster samples to improve the precision of these cosmological parameter estimates to the few percent level that Cosmic Microwave Background experiments hope to attain. For instance, a sample of 200-300 clusters, with the accompanying field, spread more or less uniformly over the  $0 < z < 1$  range would allow  $\Omega_M$  to be measured to a precision of about 2-3% and  $\Omega_\Lambda$  to be measured to about 5%. The  $\sigma_8$  parameter could be measured to a precision of better than 1%, which would become a very strong constraint on the overall spectrum of fluctuations. The galaxy evolution parameters would be measured at about 5% precision and would challenge stellar population models, and might even begin to rival globular clusters as tools to measure the age of the universe. However, this would also take some advances in modeling precision. The realistic errors are likely to be about twice as large, since new residual systematic errors will be uncovered and removed as the dataset grows. At redshifts beyond about  $z = 0.5$  the first problem is to find clusters in some systematic manner. This is mainly a matter of systematic sky surveys of various sorts. It should be noted that,

in the  $0.2 \leq z \leq 0.55$  range of the EMSS/CNOC survey, we selected only 15 clusters that are sufficiently rich that they are easy to study from 584 square degrees of sky. The implication is that these large, rich, easily-studied clusters are rather scarce on the sky. Nevertheless, once found, clusters of this sort will be exceptionally powerful as direct probes of both cosmological processes and cosmological parameters. Such programs will be feasible with a number of the new generation of telescopes.

## References

Abraham, R. G., Smecker-Hane, T. A., Hutchings, J. B., Carlberg, R. G., Yee, H. K. C., Ellingson, E., Morris, S. L., Oke, J. B., Davidge, T. 1996, ApJ, 471, 694

Baade, W. & Spitzer, L. 1951, ApJ, 113, 413

Bahcall, J. & Tremaine, S. D. 1981, ApJ, 244, 805

Bahcall, N. A., Lubin, L. M., & Dorman, V. 1995, ApJ(Lett), 447, L81

Bardeen, J. M., Steinhardt, P. J. & Turner, M. S. 1983, Phys. Rev. D., 28, 679

Binney, J. & Tremaine, S. 1987, *Galactic Dynamics*, (Princeton University Press: Princeton)

Bruzual, G. & Charlot, S. 1993, ApJ, 405, 538

Butcher, H. & Oemler, A. 1984, ApJ, 285, 423

Carlberg, R. G., Yee, H. K. C., Ellingson, E., Abraham, R., Gravel, P., Morris, S. L., & Pritchett, C. J. 1996, ApJ, 462, 32

Carlberg, R. G., Yee, H. K. C., & Ellingson, E. 1997, ApJ, in press

Carlberg, R. G., Yee, H. K. C., Ellingson, E., Morris, S. L., Abraham, R., Gravel, P., Pritchett, C. J., Smecker-Hane, T., Hartwick, F. D. A., Hesser, J. E., Hutchings, J. B., & Oke, J. B. 1997a, ApJ(Lett), 476, L7

Carlberg, R. G., Morris, S. L., Yee, H. K. C., & Ellingson, E. 1997b, ApJ, in press (astroph/9612169)

Carlberg, R. G., Cowie, L. L., Songaila, A., & Hu, E. M. 1997c, ApJ, in press (astroph/9605024)

Carlberg, R. G., Yee, H. K. C., Ellingson, E., Morris, S. L., Abraham, R., Gravel, P., Pritchett, C. J., Smecker-Hane, T., Hartwick, F. D. A., Hesser, J. E., Hutchings, J. B., & Oke, J. B. 1997d, ApJ(Lett), submitted (astroph/9703107)

Couch, W. J. & Sharples, R. M. 1987, MNRAS, 229, 423

Cole, S. & Lacey, C. G. 1996, MNRAS, in press (astroph/9510147)

David, L. P., Jones, C., & Forman, W. 1995, ApJ, 445, 578

Davis, M., Nusser, A. & Willick, J. A. 1996, ApJ, 473, 22

Dekel, A. 1994, ARAA, 32, 371

Fischer, P. & Tyson, J. A. 1997, AJ, in press (astroph/9703189)

Fisher, K. B., Davis, M., Strauss, M. A., Yahil, A., & Huchra, J. P. 1994, MNRAS, 267, 927

Gioia, I. M. & Luppino, G. A. 1994, ApJS, 94, 583

Gioia, I. M., Maccacaro, T., Schild, R. E., Wolter, Stocke, J. T., Morris, S. L., & Henry, J. P. 1990, ApJS, 72, 567

Gott, J. R. & Gunn, J. 1972, ApJ, 176, 1

Gott, J. R. & Turner, E. L. 1976, ApJ, 209, 1

Gunn, J. E. 1978, in *Observational Cosmology*, eds. Maeder, A., Martinet, L., & Tammann, G. 1978 (Geneva Observatory: Sauverny)

Guth, A. 1981, Phys. Rev. D., 23, 34

Henry, J. P., Gioia, I. M., Maccacaro, T., Morris, S. L., Stocke, J. T., & Wolter, A. 1992, ApJ, 386, 408

Hernquist, L. 1990, ApJ, 356, 359

Kennicutt, R. C. Jr. 1992, *ApJ*, 388, 310

Lilly, S. J., Tresse, L., Hammer, F., Crampton, D., & Le Fèvre, O. 1995, *ApJ*, 455, 108

Lilly, S. J., Le Fèvre, O., Hammer, F., & Crampton, D. 1996, *ApJ(Lett)*, 460, 1L

Lin, H., Yee, H. K. C., **Carlberg**, R. G., & Ellingson, E. 1997, *ApJ*, 475, 494

Luppino, G. A. & Gioia, I. M. 1995, *ApJ(Lett)*, 445, 77L

Mushotzky, R. F. & Scharf, C. A. 1997, *ApJ(Lett)*, in press (astroph/9703039)

Mazure, A., Katgert, P., den Hartog, R., Biviano, A., Dubath, P., Escalara, E., Focardi, P., Gerbal, D., Giuricin, G., Jones, B., Le Fèvre, O., Moles, M., Perea, J., & Rhee, G. 1996, *AAp*, 310, 31

Navarro, J. F., Frenk, C. S. & White, S. D. M. 1997, *ApJ*, submitted (astro-ph/9611107) NFW

Oort, J. H. 1958, in *La Structure et L'Évolution de L'Univers*, Onzième Conseil de Physique, ed. R. Stoops (Solvay: Bruxelles) p. 163

Press, W. H. & Schechter, P. 1974, *ApJ*, 187, 425

Sandage, A., Tamman, G. A., & Yahil, A. 1979, *ApJ*, 232, 352

Saunders, W., Rowan-Robinson, M., Lawrence, A., Efstathiou, G., Kaiser, N., Ellis, R. S., & Frenk, C. S. 1990, *MNRAS*, 242, 318

Schade, D., Carlberg, R. G., Yee, H. K. C., López-Cruz, O. & Ellingson, E. 1996a, *ApJ(Lett)*, 464, L63

Schade, D., Carlberg, R. G., Yee, H. K. C., López-Cruz, O. & Ellingson, E. 1996b, *ApJ(Lett)*, 465, L103

Smail, I., Ellis, R. S., Dressler, A., Couch, W. J., Oemler, A. Jr., Sharples, R. M., & Butcher, H. 1997, *ApJ*, 479, 70

Squires, G., Neumann, D. M., Kaiser, N., Fahlman, G., Woods, D., Babul, A., & Böhringer, H. 1996, *ApJ*, 469, 73

Strauss, M. A. & Willick, J. A. 1995, *Physics Reports*, 261, 271

Turner, M. 1995, *Ann. NY Acad. Sci.* 759, 153 (astroph/9703194)

Tyson, J. A. & Fischer, P. 1995, *ApJ(Lett)*, 446, 55L

Willick, J. A., Strauss, M. A., Dekel, A., & Kolatt, T. 1996, *ApJ*, submitted (astroph/9612240)

Yee, H. K. C., Ellingson, E. & Carlberg, R. G. 1996, *ApJS*, 102, 269